ACS OMEGA

Open Access

http://pubs.acs.org/journal/acsodf

Article

Two Novel Regioisomeric Series of Bis-pyrazolines: Synthesis, *In Silico* Study, DFT Calculations, and Comparative Antibacterial Potency Profile against Drug-Resistant Bacteria; MSSA, MRSA, and VRSA

Refaie M. Kassab,* Magdi E. A. Zaki, Sami A. Al-Hussain,* Aboubakr H. Abdelmonsef, and Zeinab A. Muhammad*

Cite This: *ACS Omega* 2024, 9, 3349−3362

Read Online

ACCESS | Metrics & More | Article Recommendations | Supporting Information

ABSTRACT: *Aims*: Design and synthesis of antimicrobial prototypes that are capable of eradicating bacterial biofilm formation that is responsible for many health challenges particularly with antibiotic-resistant bacterial species. *Materials and Methods*: The utility of 1,3-diarylenones, *aka* chalcones, **3a−i** and **8a−j** as building blocks to construct the corresponding bis-pyrazoline derivatives **5aa-bh** and **9ad-bj**. Screening the antibacterial behavior of the novel bis-pyrazoline derivatives against methicillin-sensitive *Staphylococcus aureus* (MSSA), methicillin-resistant *S. aureus* (MRSA), and vancomycin-resistant *S. aureus* (VRSA) bacterial strains was investigated. *Results*: Chalcones were used as building scaffolds to construct two series of di- and trisubstituted bis-pyrazoline derivatives. Numerous novel bis-compounds displayed decent bacterial biofilm suppression. *Conclusions*: Two regioisomeric series of bis-chalcones were designed and constructed, and their structural diversity was manipulated to access the intrinsically bioactive, pyrazoline ring. The newly synthesized bis-pyrazoline derivatives presented decent antibacterial behavior against multiple drug-resistant bacterial strands (MSSA, MRSA, and VRSA).

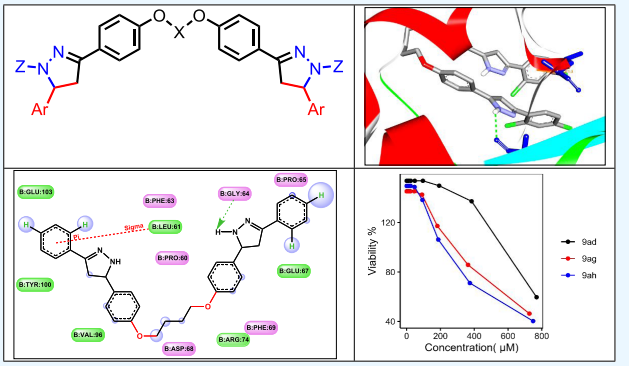

1. INTRODUCTION

Pyrazolines represent an important family in heterocyclic chemistry.[1] The pyrazoline core showcases an attractive combination of synthetic versatility as well as biological diversity.[2] The pyrazoline template is one of the most bioactive five membered rings. The pyrazoline structure can be found in various clinically used drugs (Figure 1).

Many pyrazoline derivatives have been reported as antimicrobial,[3] antifungal,[4] antimalarial,[5] antiamoebic,[6] anti-inflammatory,[7] anticancer,[8] antidepressant,[9] anticonvulsant,[10] and/or antitubercular.[11] Other pyrazolines were reported as EGFR tyrosine kinase inhibitors[12] and cannabinoid CB1 receptor agonists.[13]

The biological profile of pyrazolines is dramatically correlated with the relative substitution pattern, especially at N-1, C-3, and C-5 positions. Similar to many other bis-heterocyclic compounds,[14−19] designing new classes of bis-3,5-diaryl pyrazolines has been attracting an increased attention over the last couple of decades due to their potential biological and pharmacological applications.[17−21] Like their parent heterocyclic pyrazolines, bis-3,5-diaryl pyrazoline derivatives, their bis-heterocyclic analogues, have been known for their high bioactive threshold. Many bioactive bis-3,5-diaryl pyrazolines were constructed from bis-1,3-diarylenone precursors.[22−25]

1,3-Diarylenones, *aka* bis-chalcones, are synthetically versatile scaffolds[26−28] that could exhibit a host of bioactivities themselves, including antibacterial,[29] fungicidal,[30] and antimalarial.[31]

In this report, we are expanding the synthetic pool of 1,3-diarylenones by adding two new groups of bis-enones, examining the bioactive capacity of these bis-enones themselves, and ultimately using their structural assortment to access two more series of the biologically active pyrazoline core. Herein, we present the synthesis of two new isomeric series of di- and triaryl bis-pyrazoline derivatives besides their antibacterial potency outline versus some chosen drug-resistant bacterial strands; methicillin-sensitive *Staphylococcus aureus* (MSSA), methicillin-resistant *S. aureus* (MRSA), and vancomycin-resistant *S. aureus*

Received: August 25, 2023
Revised: December 18, 2023
Accepted: December 21, 2023
Published: January 9, 2024

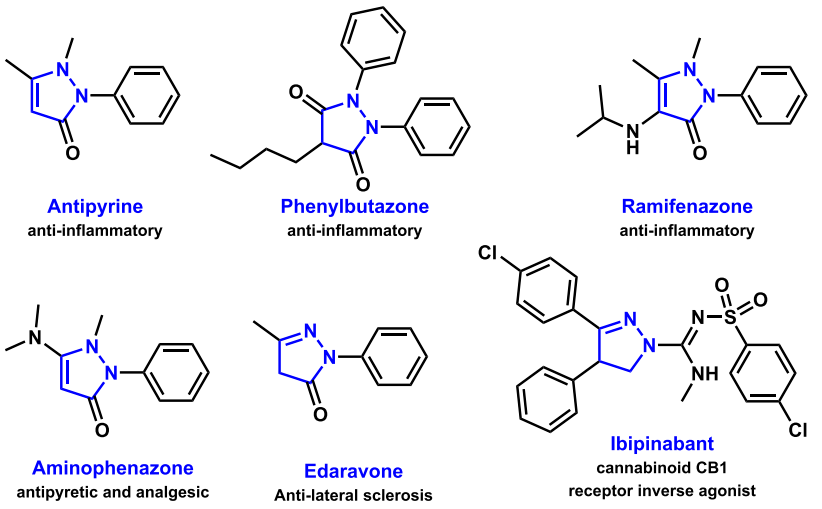

Figure 1. Some pyrazoline-based drugs.

Scheme 1. Synthesis of Bis-chalcone Derivatives 3a−i

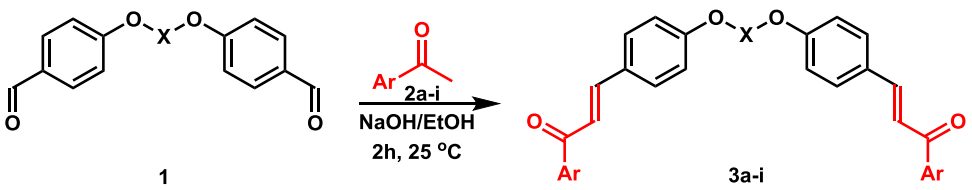

Compound	Ar	%Yield
3a	C_6H_5	80
3b	4-$CH_3C_6H_4$	84
3c	2-ClC_6H_4	68
3d	4-ClC_6H_4	74
3e	2-BrC_6H_4	68
3f	4-BrC_6H_4	93
3g	2-$NO_2C_6H_4$	79
3h	4-$NO_2C_6H_4$	61
3i	4-$NH_2C_6H_4$	77
X= $(CH_2)_4$		

(VRSA). Special attention was directed to the effect of changing the substitution pattern at the N-1, C-3, and C-5 positions of the pyrazolidine ring and its direct correlation with the biological profile of the newly synthesized bis-pyrazolidine derivatives against any of the screened drug-resistant bacterial strands. The cytotoxicity of the new bis-pyrazoline derivatives as well as their effect on bacterial biofilm formation were also studied. Molecular docking simulations, density functional theory-absorption, distribution, metabolism, excretion and toxicity (DFT-ADMET) calculations, electrostatic potential (ESP) map, and drug structural activity relationship (SAR) were conducted to describe the intermolecular interactions and to predict the plausible mode(s) of action between the bis-pyrazoline derivatives and the target bacterial enzyme.

2. RESULTS AND DISCUSSION

2.1. Chemistry. A new series of bis-chalcone derivatives **3a−i** were prepared from the conventional base-catalyzed aldol condensation of one equivalent of the bis-aldehyde **1** with two equivalents of a series of methyl aryl ketone, *aka* acetophenones, **2a−i** in sodium hydroxide ethanolic blend (NaOH/EtOH) (Scheme 1). All proposed chemical structures of the newly formed chalcones **3a−i** were elucidated by their spectral and elemental analyses. The ketone−enone transformation was evidenced by a drop in carbonyl stretch from 1680−1705 to 1650−1670 cm^{-1} (IR spectra). The ^1H NMR spectra contained two doublets at δ = 7.80−7.85 and 7.90−8.00 typical for the two olefinic protons. Moreover, the sole formation of the *E*-enone was established based on its vicinal *J*-value of 15−16 Hz (see Section 4).

https://doi.org/10.1021/acsomega.3c06348
ACS Omega 2024, 9, 3349−3362

Scheme 2. Synthesis of Bis-pyrazoline Derivatives 5aa-bh

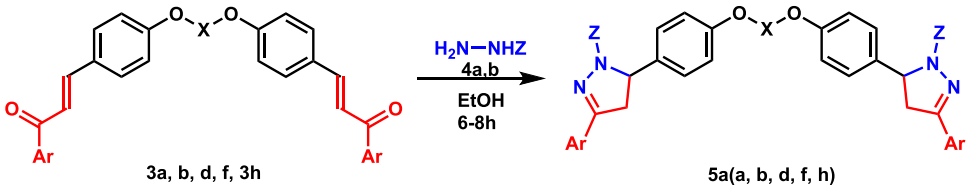

Compound		Z	Yield %
5aa	C_6H_5	**H**	80 %
5ab	4-$CH_3C_6H_4$	**H**	78 %
5ad	4-ClC_6H_4	**H**	84 %
5af	4-BrC_6H_4	**H**	86 %
5ah	4-$NO_2C_6H_4$	**H**	75 %
5ba	C_6H_5	**Ph**	76 %
5bb	4-$CH_3C_6H_4$	**Ph**	70 %
5bd	4-ClC_6H_4	**Ph**	82 %
5bf	4-BrC_6H_4	**Ph**	80 %
5bh	4-$NO_2C_6H_4$	**Ph**	72 %
	X= $(CH_2)_4$		

Scheme 3. Synthesis of Bis-chalcone Derivatives 8a−j

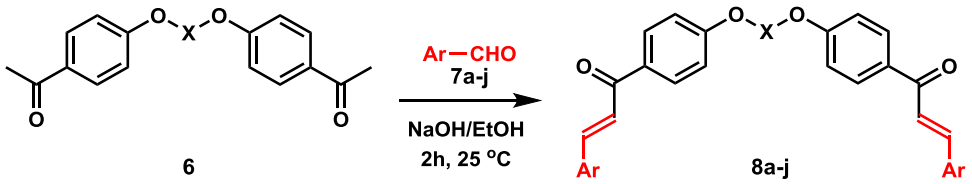

Compound	Ar	% Yield
8a	C_6H_5	77
8b	4-$CH_3C_6H_4$	75
8c	4-$OCH_3C_6H_4$	68
8d	3,5-$OCH_3C_6H_3$	60
8e	3,4,5-$OCH_3C_6H_2$	65
8f	4-ClC_6H_4	90
8g	4-BrC_6H_4	85
8h	2,4-ClC_6H_3	80
8i	4-$NO_2C_6H_4$	70
8j		80
	X= $(CH_2)_4$	

A series of new pyrazoline derivatives **5a(a, b, d, f, h)** and phenyl pyrazoline **5b(a, b, d, f, h)** were then synthesized from the reaction of two equivalents of hydrazine hydrate or phenyl hydrazine, respectively, with a series of various chalcones **3a, b, d, f, and h** in refluxing 6−8 h (Scheme 2). The chemical structures of all newly formed bis-pyrazolines, **5a(a, b, d, f, h) and 5b(a, b, d, f, h)**, were assured and established on their spectral and elemental analyses. Their infrared (IR) spectra of newly formed bis-pyrazoline **5a(a, b, d, f, h)** were found to be free from any characteristic C═O signal and revealed the NH

https://doi.org/10.1021/acsomega.3c06348
ACS Omega 2024, 9, 3349−3362

Scheme 4. Synthesis of Bis-pyrazoline Derivatives 9ad-bj

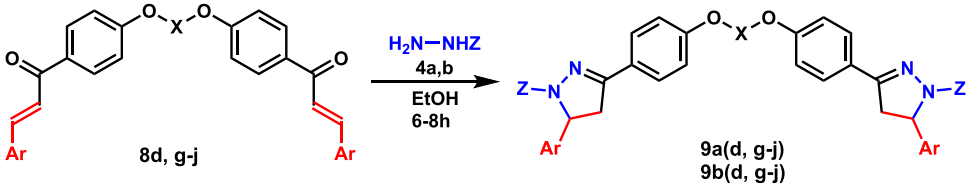

Compound	Ar	Z	% Yield
9ad	3,5-$OCH_3C_6H_3$	**H**	72
9ag	4-BrC_6H_4	**H**	70
9ah	2,4-ClC_6H_3	**H**	75
9ai	4-$NO_2C_6H_4$	**H**	65
9aj		**H**	68
9bd	3,5-$OCH_3C_6H_3$	**Ph**	72
9bg	4-BrC_6H_4	**Ph**	70
9bh	2,4-ClC_6H_3	**Ph**	65
9bi	4-$NO_2C_6H_4$	**Ph**	60
9bj		**Ph**	66

Table 1. MIC (μM) Values of Bis-pyrazoline Derivatives against Various Bacterial Species

A. methicillin-sensitive *S. aureus* (MSSA) ATCC 29213		B. methicillin-resistant *S. aureus* (MRSA) ATCC 700788		C. vancomycin-resistant *S. aureus* (VRSA) RCMB 28354	
compound	MIC	compound	MIC	compound	MIC
5aa	14.7	**5aa**	58.96	**5aa**	>1000
5ab	13.9	**5ab**	28.01	**5ab**	896
5ad	0.40	**5ad**	1.63	**5ad**	13.03
5af	5.60	**5af**	11.35	**5af**	90.8
5ah	1.51	**5ah**	3.14	**5ah**	25.20
5ba	0.71	**5ba**	2.85	**5ba**	22.91
5bb	10.9	**5bb**	21.89	**5bb**	na
5bd	20.8	**5bd**	41.60	**5bd**	na
5bf	4.60	**5bf**	18.60	**5bf**	297.61
5bh	80.9	**5bh**	na	**5bh**	na
9ad	0.36	**9ad**	1.50	**9ad**	6.00
9ag	0.71	**9ag**	1.42	**9ag**	11.35
9ah	0.17	**9ah**	0.71	**9ah**	5.83
9ai	25.2	**9ai**	100.80	**9ai**	na
9aj	3.82	**9aj**	15.31	**9aj**	61.27
9bd	1.22	**9bd**	4.86	**9bd**	na
9bg	9.29	**9bg**	18.60	**9bg**	na
9bh	1.19	**9bh**	2.37	**9bh**	9.52
9bi	10.11	**9bi**	40.47	**9bi**	na
9bj	5.89	**9bj**	23.61	**9bj**	188.8
vancomycin	0.338	**vancomycin**	1.345	**vancomycin**	nd

absorption bands and ═C−H stretches at $\dot{\upsilon}$ = 1653−1668 and 2964−3110 cm^{-1}, respectively. Also, ^{1}H NMR of all isolated bis-pyrazoline **5b(a, b, d, f, h)** showed all presumed signals for the indicated structure. Compound **5ab**, for instance, showed the expected signals at 1.85 (t, 4H, $2CH_2$), 3.36 (t, 2H, CH, pyrazoline-H), 4.00 (t, 4H, $2CH_2$), 4.81−4.78 (t, 4H, $2CH_2$, pyrazoline), 6.87−7.52 (m, 16H, Ar−H), and 7.97 (s, 2H, 2NH) ppm. Moreover, compound **5ab** had 14 nonequivalent carbon signals in its ^{13}C NMR spectrum (see Section 4).

https://doi.org/10.1021/acsomega.3c06348
ACS Omega 2024, 9, 3349−3362

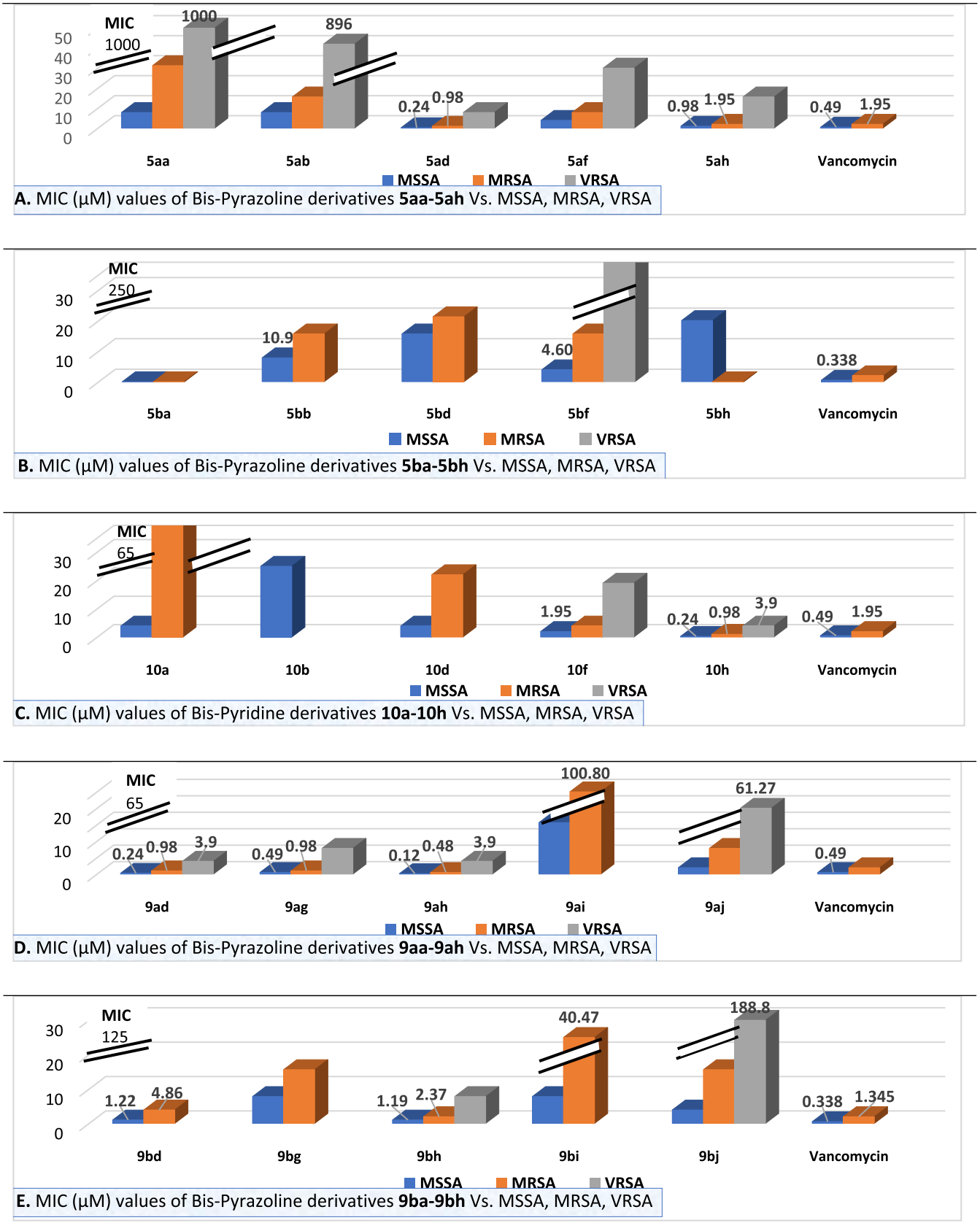

Figure 2. MIC values of some bis-pyrazolidine and bis-pyridene derivatives vs. MSSA, MRSA, and VRSA.

A series of novel chalcone derivatives **8a−j** were prepared from the classical base-catalyzed aldol condensation of one equivalent of bis-ketone **6** with two equivalents of a group of aldehydes **7a−j** in ethanolic mixture of NaOH as the basic catalyst (Scheme 3). The chemical structure of all freshly prepared bis-enone derivatives **8a−j** was easily established based

https://doi.org/10.1021/acsomega.3c06348
ACS Omega 2024, 9, 3349−3362

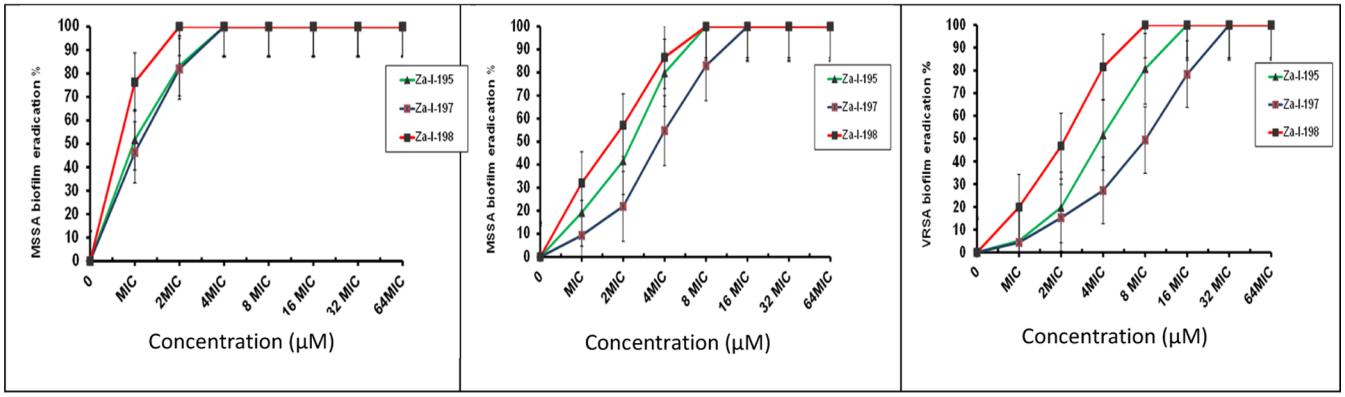

Figure 3. Biofilm eradication activities of compounds **9ad** (green), **9ag** (blue), and **9ah** (red) against MSSA, MRSA, and VRSA bacterial strains. The tick labels on the *x*-axis indicate the concentration of the compound in units of MIC (*i.e.*, 1 = 1 MIC, 2 = 2 MIC, etc.).

on their spectral and elemental analyses. As projected, the IR spectra demonstrated a typical drop in the carbonyl stretching absorption from 1651−1689 cm^{-1}, representative for acetophenones, to 1640−1670 cm^{-1}, distinctive for enones. The ^1H NMR spectra contained a pair of doublets at δ = 6.99−7.12 and 8.13−8.25 distinctive for the two olefinic protons. Additionally, the sole formation of the *E*-enone was idicated by a vicinal *J*-value of 15−16 Hz (see Section 4).

A series of new pyrazoline derivatives **9a(d, g-j)** and phenyl pyrazolines **9b(d, g-j)** were then synthesized from the reaction of two equivalents of hydrazine hydrate or phenyl hydrazine, respectively, with bis-chalcone derivatives **8** in boiling ethanol for 6−8 h (Scheme 4). The chemical framework of all newly formed bis-pyrazoline **9a(d, g-j)** and phenyl pyrazoline **9b(d, g-j)** was established by their spectral and elemental analyses. Their IR spectra of newly formed bis-pyrazoline **9a(d, g-j)** and phenyl pyrazoline **9b(d, g-j)** were found to be free from any characteristic C═O signal and revealed the NH absorption bands and ═C−H stretches at $\acute{\upsilon}$ = 3332−2240 and 2939−3101 cm^{-1}, respectively. Also, ^1H NMR of all isolated bis-pyrazoline **9a(d, g-j)** showed all anticipated signals for the submitted structure. Compound **9ad**, for instance, showed signals at 1.90 (t, 4H, $2CH_2$), 3.84 (t, 2H, CH, pyrazoline-H), 4.15 (t, 4H, $2CH_2$), 4.81−4.78 (t, 4H, $2CH_2$, pyrazoline), 6.94−8.13 (m, 14H, Ar−H), and 7.16 (s, 2H, 2NH) ppm (see Section 4).

The spectral analyses of all compounds are included in the supplementary data file as Figures S1−S75.

2.2. Biological Study. *2.2.1. Assessment of Antimicrobial Activity and MIC Determination.* The antimicrobial activity of the new bis-pyrazolines was screened versus methicillin-sensitive *S. aureus* (*MSSA*) *ATCC 29213*, methicillin-resistant *S. aureus* (*MRSA*) *ATCC 700788*, and vancomycin-resistant *S. aureus* (*VRSA*) *RCMB 28354* using the cup-plate method. It is noteworthy to point out that Gram-negative bacteria display a higher degree of resistance to antimicrobial agents compared to Gram-positive bacteria. The enhanced drug resistance that Gram-negative bacteria possess can be attributed to the presence of an outer membrane, which provides an additional layer of protection and serves as a distinctive barrier that impedes the penetration of antibiotics into the cell wall.

The compounds that have shown inhibition zones were additionally screened for MIC using broth microdilution technique. The MIC values of the examined compounds are recorded in Table 1.

Upon screening the new bis-pyrazoline derivatives against (*MSSA*) *ATCC 29213*, the popular delegate of Gram-negative pathogens, compounds **5ba** and **9ag** had equal MIC values as vancomycin (MIC_{Vanc}). While compounds **5ad** and **9ad** had MIC value of one-half of that of MIC_{Vanc} (Table 1A and Figure 2). Similarly, upon screening the new bis-pyrazoline derivatives vesus (*MRSA*) *ATCC 700788*, the popular delegate of Gram-negative pathogens, compounds **5ah, 5ba**, and **9ah** had MIC values of quadruple that of vancomycin (MIC_{Vanc}). While compounds **5ad**, **9ad**, and **9ag** had MICs double that of MIC_{Vanc}. However, compound **9ah** had the lowest MIC value of only one-fourth the MIC_{Vanc} (Table 1B and Figure 2). Finally, upon screening the new pyrazoline derivatives against (*VRSA*) *RCMB 28354*, compounds **9ad** and **9ah** showed the lowest MIC value of 6 and 5.83 μM. (Table 1C and Figure 2).

From the above data analysis, one could easily conclude that compounds **9ad**, **9ag**, and **9ah** are the most potent pyrazolines against all three screened bacterial strands; MSSA, MRSA, and VRSA.

It is worth mentioning that we have recently reported the synthesis of some bis-pyridine derivatives that exhibited high potency against the three screened bacterial strands; MSSA, MRSA, and VRSA (Figure 2C).[32] However, bis-pyrazoline derivatives **9ad**, **9ag**, and **9ah** exhibit higher potency when compared to their bis-pyridine counterparts.

2.2.2. Comparative Structure Activity Relationship (SAR). In this section, special consideration was geared toward the effect of changing the substitution pattern at the N-1, C-3, and C-5 positions of the pyrazoline ring system and its correlation with the biological activities of the newly synthesized bis-pyrazoline derivatives against any of the screened drug-resistant bacterial strands, MSSA, MRSA, or VRSA.

Our preliminary study on the structure activity relationship (SAR) using the information presented in Table 1 and Graph 3 revealed several observations. For series **5aa-5ah**, the more electron-deficient the Ar pendant in the pyrazolidine ring becomes, the smaller the MIC value, with compounds **5ad** and **5ah** showing the highest potency with low MIC values of 0.40 and 1.50, respectively.

Recently, we have reported a similar MIC pattern[32] with comparable bis-pyridine series where compound **10h** had an MIC value of 2.51 for MSSA and compound **10f** had MIC values of 0.27, 1.10, and 4.41 for MSSA, MRSA, and VRSA, respectively.

However, for the more sterically congested series **5ba-5bh**, the less electron-deficient the Ar pendant in the pyrazolidine ring becomes, the smaller the MIC value, with compound **5ba**

https://doi.org/10.1021/acsomega.3c06348
ACS Omega 2024, 9, 3349−3362

showing the highest potency with low MIC values of 0.71 and 2.85 for MSSA and MRSA, respectively.

For series **9aa-9aj**, as the Ar pendant in the pyrazolidine ring becomes more electron-rich, the smaller the MIC value, with compounds **9ad**, **9ag**, and **9ah** showing the highest potency, with lower MIC values across the border for MSSA, MRSA, and VRSA.

However, for the more sterically congested series **9ba-9bj**, there was no steady correlation between the electronics of the Ar pendant in the pyrazolidine ring and the recorded MIC values, *i.e.*, the potency against any of the screened drug-resistant bacterial strands, MSSA, MRSA, or VRSA.

2.2.3. Effect on Biofilm Formation. Bacterial biofilm formation constitutes an alternative lifestyle by which specific bacteria can embrace a multicellular comportment that extends their existence in different ecological situations.[33] Bacterial biofilm formation on hospital equipment represents a major health hazard if transferred to patients. Contained by the human host, bacterial biofilms aid bacterial cells to resist the immune system. Consequently, building new materials that could eliminate bacterial biofilm formation is essential to avoid some serious health problems.

Compounds with MIC values analogous to that of vancomycin were additionally inspected, at 50% of their MIC values, as potential antibiofilm prototypes (Figure 3). Upon examining bis-pyrazolines **9ad**, **9ag**, and **9ah** against biofilm formation by *S. aureus* (MSSA) ATCC 29213, these compounds presented lowest biofilm inhibitory concentrations of *ca.* 1.47, 2.84, and 0.35 μg/mL while vancomycin demonstrated *ca.* 32 μM (Table 2 and Figure 3). Bis-pyrazolines **9ad**, **9ag**, and **9ah** also showed biofilm inhibitory concentrations of *ca.* 12.06, 22.79, and 5.74 μM, respectively, when examined against *S. aureus* (MRSA) ATCC 700788 biofilm. However, an MIC concentration of 64 μM of vancomycin was required to eradicate biofilm formation by MRSA. These results could suggest the supremacy of halogen-substituted compounds for destroying bacterial biofilm structure (Table 2 and Figure 3).

Table 2. Minimum Biofilm Eradication Concentration of Compounds 9ad, 9ag, and 9ah Compared to Standard Vancomycin against MSSA, MRSA, and VRSA Bacterial Strains

	MIC (μM)			
pathogens	**9ad**	**9ag**	**9ah**	vancomycin
MSSA	1.47 (4 MIC)	2.81 (4 MIC)	0.35 (2 MIC)	10.82 (32 MIC)
MRSA	12.06 (8 MIC)	22.79 (16 MIC)	5.74 (8 MIC)	86.12 (64 MIC)
VRSA	96 (16 MIC)	363.25 (32 MIC)	46.70 (32 MIC)	nd

2.2.4. Cytotoxicity on Normal WI-38 Cell Line. The results offered in Section 2.3 denote that the examined compounds have an effective inhibitory action on bacterial cells at the test concentration. To assess the biocompatibility of these test compounds with typical human cells, the cytotoxicities of compounds **9ad**, **9ag**, and **9ah** were checked *via* the MTT assay. The results presented in Figure 4 portray that the three examined compounds have high CC_{50} (cytotoxic concentrations) values (351.79−693.54 μM) compared to the standards required to prevent bacterial biofilm formation (2−4 μM, Figure 4), signifying their biocompatibility with regular human lung fibroblast cells (WI-38). Accordingly, the synthesized compounds could be encouraging prototypes for potential bacterial biofilm suppression within biological frameworks.

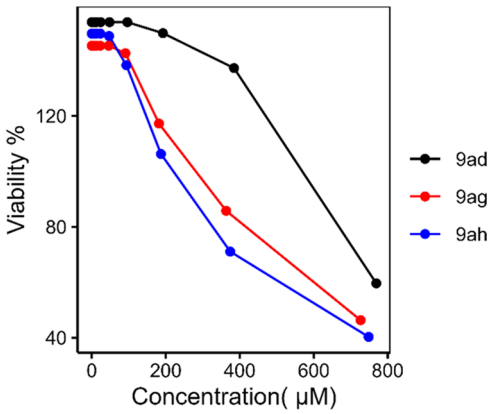

Figure 4. Cytotoxicity test of compounds **9ad** (black), **9ag** (red), and **9ah** (blue) on normal human lung fibroblast cells. The obtained CC_{50} values are 693.54 ± 31.8, 495.63 ± 27.6, and 351.79 ± 19.1 μM for compounds **9ad**, **9ag**, and **9ah**, respectively.

2.3. Molecular Docking Approach and ADMET Analysis. To check the affinity of the newly synthesized bis-pyrazoline derivatives against methicillin-resistant *S. aureus* (MRSA), a molecular docking study was performed.[34−36] The minimum binding energy confirmed that the target was successfully docked with the ligand molecules. The obtained data suggested that the studied bis-pyrazoline derivatives were fit docked to the effective site pockets of the host in the range of −13.1 to −12.7 kcal/mol. The docking energies for the best docked compounds and intermolecular bond lengths are summarized in Table 3. two-dimensional (2D) and three-dimensional (3D) demonstrations of interaction maps of the best enzyme−ligand docked complexes are exemplified in Figure 5. Compound **9ad** (with two electron-donating MeO− groups) has the best binding energy = −13.1 kcal/mol *via* docking to the target enzyme *via* one H-bond interaction with Phe63 at 2.40 Å. Moreover, compound **9ag** docked to the target through H-bond with Leu61. However, compound **9ah** docked to the target through one H-bond and arene-sigma interactions with Glys64 and Leu61 at 2.11 and 3.89 Å, respectively. Furthermore, electrostatic potential map of compound **9ah** showed that the aromatic rings have high electronegative charge than the other side chain of the molecule, confirming high ability to bind by the dynamic site of the target enzyme, as displayed in Figure 6.

Table 3. Binding Energies of the Best Docked Compounds

	binding energy kcal/mol	docked complex (amino acid−ligand) interactions	distance (Å)
9ad	−13.1	H-bonds	2.40
		PHE63:O—compound **9ad**	
9ag	−12.9	H-bonds	2.15
		Leu61:O—compound **9ag**	
9ah	−12.7	H-bonds	2.11
		Gly64:O—compound **9ah**	
		arene-sigma	3.89
		PHE63—compound **9ah**	

To predict the druggability of the synthesized compounds, ADMET and pharmacokinetic properties were evaluated. The obtained results suggested that all compounds could potentially

https://doi.org/10.1021/acsomega.3c06348
ACS Omega 2024, 9, 3349−3362

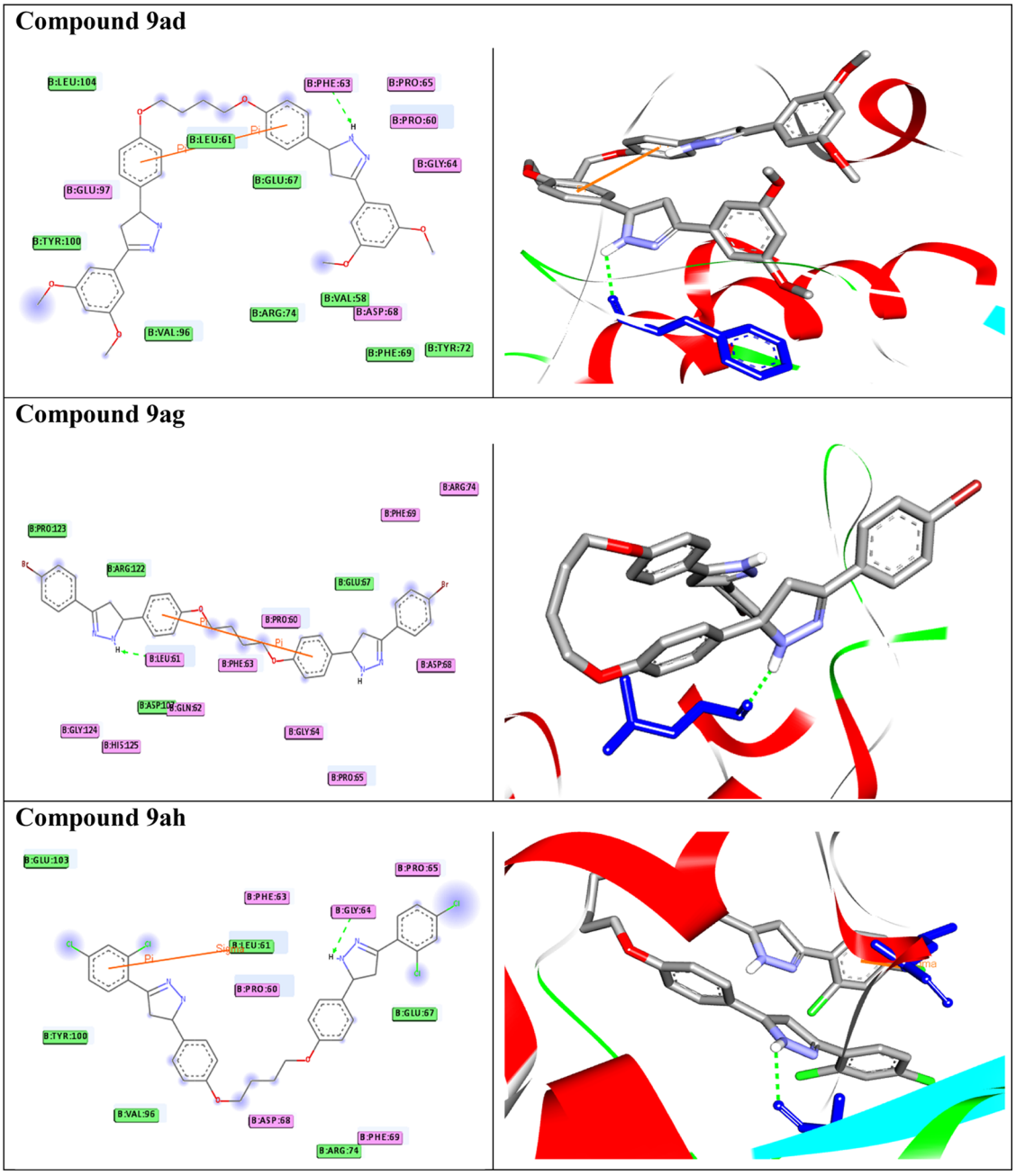

Figure 5. 2D and 3D representation of intermolecular interactions between the best docked compounds and MRSA enzyme.

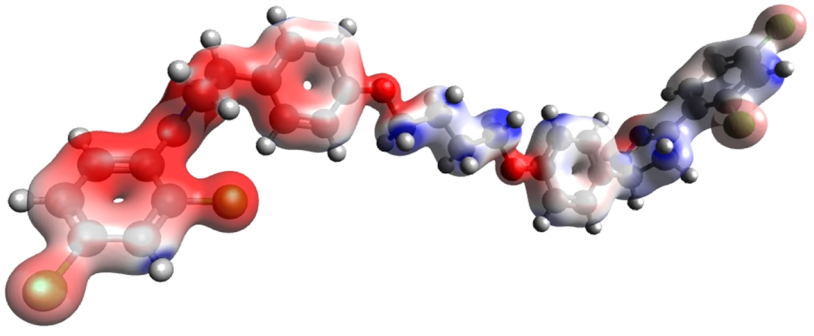

Figure 6. Spatial electrostatic potential (ESP) map of compound **9ah**. Red and blue zones represented high and low electronegative sides, respectively.

be well-absorbed *via* the intestinal barrier but not at the level of the blood−brain barrier. Finally, compounds **9ad**, **9ag**, and **9ah** obeyed the Lipinski rule of five (Ro5), by not having more than one violation, as shown in Table 4.

https://doi.org/10.1021/acsomega.3c06348
ACS Omega 2024, 9, 3349−3362

Table 4. ADMET Analysis of the Best Docked Compounds

	molecular weight (g/mol)	% (HIA+)	logp	TPSA A^2	HBA	HBD	N violations	volume A^3			
reference range	130−500	<25 poor >80 high	<5	≤140	2−20	0−6	<5	500−2000	GI absorption	bio-availability score	BBB permeant
9ad	650.76	98.98	3.13	104.16	8	2	1	602.53	high	0.55	no
9ag	688.45	99.67	5.00	67.24	4	2	1	536.12	high	0.17	no
9ah	668.44	100.00	3.26	67.24	4	2	1	554.49	low	0.17	no

3. CONCLUSIONS

Two contemporary series of bis-enones, *aka* bis-chalcones, with innate bioactive capacity were designed. The natural bioactive capacity of the new bis-enones was exploited to manipulate their basic assortment to construct the more biologically dynamic pyrazoline core. Thus, two new regioisomeric sets of di- and trisubstituted bis-pyrazoline derivatives were successfully synthesized. The newly synthesized bis-pyrazoline derivatives presented satisfactory antibacterial performance counter to several drug-resistant bacterial species; namely, MSSA, MRSA, and VRSA. The study of structural-activity relationships revealed that the chalcone series that was formed *via* condensation of bis-acetophenones with electron-rich aldehydes gave more potent antibacterial prototypes of bis-pyrazolines, *e.g.*, **9ad**, **9ag**, and **9ah**.

Molecular docking studies of the more effective compounds, **9ad**, **9ag**, and **9ah**, toward MRSA-PBP2a receptor projected that the possible antibacterial mechanism of action was cell wall biosynthesis inhibition. Molecular docking and molecular structure results agreed with the acquired experimental data. Generally, these results specified that bis-pyrazoline **9ad**, **9ag**, and **9ah** act as PBP2a blockers and could possibly be used to eliminate drug-resistant bacteria; MSSA, MRSA, and VRSA. Additional screening of the full spectrum of the newly constructed bis-compounds; bis-enones and bis-pyrazoline, and their complete biological profile are presently under further exploration.

4. EXPERIMENTAL SECTION

4.1. Chemistry. Melting points were measured on a Gallenkamp system and were not corrected. IR spectra were collected in potassium bromide (KBr) using a Pye-Unicam SP300 spectrophotometer. ^{1}H and ^{13}C NMR spectra were collected in deuterated DMSO-d_6 using a Varian Gemini 300 NMR spectrometer (300 MHz for ^{1}H NMR and 75 MHz for ^{13}C NMR), and the chemical shifts were conveyed to that of the solvent DMSO-d_6. Mass spectra were collected on GCMS-Q1000-EX Shimadzu and GCMS 5988-A HP spectrometers using 70 eV ionizing voltage. Elemental analyses were performed at the Microanalytical Centre of Cairo University, Giza, Egypt. Biological assessments were performed at the Regional Center for Mycology and Biotechnology at Al-Azhar University, Cairo, Egypt. Compounds **3a−i** were synthesized according to a reported procedure.[32]

4.1.1. General Procedure for the Synthesis of Bis-(pyrazoline) Derivatives ***5a(a, b, d, f, h)*** *and* ***5b(a, b, d, f, h)***. A mixture of bis-chalcone derivatives **3a, b, d, e, and f** (10 mmol), hydrazine hydrate **4a**, and phenyl hydrazine **4b** (20 mmol) in ethanol (50 mL) was stirred under reflux for 6 h. The mixture was left to cool to room temperature, and the solvent was removed under vacuum. The solid product was collected, rinsed with ethanol (20 mL), air-dried, and purified by recrystallization from DMF to afford the corresponding bis(pyrazoline) derivative **5a(a, b, d, f, h) and 5b(a, b, d, f, h)**.

*4.1.2. 1,4-Bis(4-(3-phenyl-4,5-dihydro-1H-pyrazol-5-yl)-phenoxy)butane (**5aa**).* Off-white solid, 80% yield; mp 195−196 °C; IR (KBr): v 3332 (2NH), 3032, 2947 (C−H), 1674 (COO), 1350, 1249, 1172, 1056 ($4CH_2$) cm^{-1}; ^{1}H NMR (DMSO-d_6): δ 1.94 (t, 4H, $2CH_2$), 3.31 (t, 2H, CH, pyrazoline-H), 4.10 (t, 4H, $2CH_2$), 4.79 (t, 4H, $2CH_2$, pyrazoline), 7.01−8.17 (m, 18H, Ar−H), 7.26 (s, 2H, 2NH) ppm; ^{13}C NMR (DMSO-d_6): δ 22.5, 25.5 ($2CH_2$), 64.5, 67.5 ($2OCH_2$), 115.2, 124.8, 126.0, 129.1, 130.0, 135.4, 136.4, 149.5, 158.0 (Ar−H) ppm; MS *m*/*z* (%): 530 (M^+, 14), 524 (66), 484 (43), 443 (86), 429 (88), 382 (73), 366 (53), 350 (50), 323 (100), 303 (61), 290 (45). Anal. calcd for $C_{34}H_{34}N_4O_2$ (530.67): C, 76.95; H, 6.46; N, 10.56. Found: C, 77.25; H, 6.30; N, 10.35%.

*4.1.3. 1,4-Bis(4-(3-(p-tolyl)-4,5-dihydro-1H-pyrazol-5-yl)-phenoxy)butane (**5ab**).* Off-white solid, 78% yield; mp 175−176 °C; IR (KBr): v 3332 (2NH), 3032, 2947 (C−H), 1350, 1249, 1172, 1111 ($4CH_2$) cm^{-1}; ^{1}H NMR (DMSO-d_6): δ 1.83 (t, 4H, $2CH_2$), 3.36 (t, 2H, CH, pyrazoline-H), 4.00 (t, 4H, $2CH_2$), 4.81−4.78 (t, 4H, $2CH_2$, pyrazoline), 6.87−7.52 (m, 16H, Ar−H), 7.97 (s, 2H, 2NH) ppm; MS *m*/*z* (%): 558 (M^+, 28), 555 (80), 554 (100), 518 (39), 479 (31), 451 (35), 431 (55), 374 (63), 363 (27), 311 (18), 246 (12), 156 (11), 103 (14), 83 (12). Anal. calcd for $C_{36}H_{38}N_4O_2$ (558.73): C, 77.39; H, 6.86; N, 10.03. Found: C, 77.60; H, 6.68; N, 9.86%.

*4.1.4. 1,4-Bis(4-(3-(4-chlorophenyl)-4,5-dihydro-1H-pyrazol-5-yl)phenoxy)butane (**5ad**).* Off-white solid, 84% yield; mp 159−160 °C; IR (KBr): v 3332 (2NH), 3039, 2948 (C−H), 1396, 1250, 1272, 1095 ($4CH_2$) cm^{-1}; ^{1}H NMR (DMSO-d_6): δ 1.87 (t, 4H, $2CH_2$), 4.16 (t, 2H, CH, pyrazoline-H), 4.00 (t, 4H, $2CH_2$), 4.81−4.88 (t, 4H, $2CH_2$, pyrazoline), 6.88−8.17 (m, 16H, Ar−H), 7.11 (s, 2H, 2NH) ppm; ^{13}C NMR (DMSO-d_6): δ 25.0, 26.8 ($2CH_2$), 62.5, 66.5 ($2OCH_2$), 114.2, 125.5, 127.4, 130.5, 131.8, 136.3, 137.5, 148.2, 159.6 (Ar−H) ppm; MS *m*/*z* (%): 601 (M+2, 11), 599 (M^+, 19), 485 (35), 448 (59), 415 (86), 332 (100), 326 (34), 306 (49), 224 (49), 176 (24), 104 (26), 44 (38). Anal. calcd for $C_{34}H_{32}Cl_2N_4O_2$ (599.56): C, 68.12; H, 5.38; N, 9.33. Found: C, 68.32; H, 5.10; N, 9.12%.

*4.1.5. 1,4-Bis(4-(3-(4-bromophenyl)-4,5-dihydro-1H-pyrazol-5-yl)phenoxy)butane (**5af**).* Off-white solid, 86% yield; mp 150−151 °C; IR (KBr): v 3332 (2NH), 3062, 2947 (C−H), 1303, 1249, 1172, 1058 ($4CH_2$) cm^{-1}; ^{1}H NMR (DMSO-d_6): δ 1.91 (t, 4H, $2CH_2$), 3.16 (t, 2H, CH, pyrazoline-H), 4.16 (t, 4H, $2CH_2$), 4.85−4.98 (t, 4H, $2CH_2$, pyrazoline), 6.91−8.16 (m, 16H, Ar−H), 7.56 (s, 2H, 2NH) ppm; MS *m*/*z* (%): 688 (M^+, 10), 649 (27), 610 (12), 573 (17), 566 (30), 510 (36), 499 (14), 441 (17), 412 (32), 407 (80), 378 (51), 362 (100), 340 (88), 318 (83), 263 (51), 248 (77), 204 (66), 165 (24), 111 (45). Anal. calcd for $C_{34}H_{32}Br_2N_4O_2$ (688.46): C, 59.32; H, 4.69; N, 8.14. Found: C, 59.50; H, 4.44; N, 7.94%.

*4.1.6. 1,4-Bis(4-(3-(4-nitrophenyl)-4,5-dihydro-1H-pyrazol-5-yl)phenoxy)butane (**5ah**).* Off-white solid, 75% yield; mp

https://doi.org/10.1021/acsomega.3c06348
ACS Omega 2024, 9, 3349−3362

174−175 °C; IR (KBr): v 3410 (2NH), 3055, 2931 (C−H), 1396, 1242, 1165, 1111 (4CH_2) cm^{-1}; ^{1}H NMR (DMSO-d_6): δ 1.85 (t, 4H, 2CH_2), 2.81 (t, 2H, CH, pyrazoline-H), 4.00 (t, 4H, 2CH_2), 4.73−4.78 (t, 4H, 2CH_2, pyrazoline), 6.88−8.16 (m, 16H, Ar−H), 10.21 (s, 2H, 2NH) ppm; ^{13}C NMR (DMSO-d_6): δ 21.3, 25.8 (2CH_2), 63.5, 67.5 (2OCH_2), 114.8, 125.8, 128.1, 129.5, 131.0, 135.3, 137.9, 149.2, 158.2 (Ar−H) ppm; MS m/z (%): 620 (M^+, 12), 576 (18), 417 (100), 378 (38), 363 (85), 317 (38), 274 (42), 262 (57), 151 (40), 104 (21), 88 (45), 43 (40). Anal. calcd for $C_{34}H_{32}N_6O_6$ (620.67): C, 65.80; H, 5.21; N, 13.53. Found: C, 66.05; H, 4.97; N, 13.25%.

*4.1.7. 1,4-Bis(4-(1,3-diphenyl-4,5-dihydro-1H-pyrazol-5-yl)phenoxy)butane (**5ba**).* Off-white solid, 76% yield; mp 209−110 °C; IR (KBr): v 3055, 2924 (C−H), 1388, 1242, 1172, 1064 (4CH_2) cm^{-1}; ^{1}H NMR (DMSO-d_6): δ 1.78 (t, 4H, 2CH_2), 3.03 (t, 2H, CH, pyrazoline-H), 3.90 (t, 4H, 2CH_2O), 5.36 (t, 2H, 2CH, pyrazoline-H), 6.66−7.74 (m, 28H, Ar−H) ppm; ^{13}C NMR (DMSO-d_6): δ 26.8, 45.8 (2CH_2), 63.5, 65.4 (2OCH_2), 111.4, 113.3, 115.2, 125.1, 127.7, 129.1, 129.3, 130.9, 133.0, 135.6, 144.8, 145.5, 155.8 (Ar−H) ppm; MS m/z (%): 682 (M^+, 14), 646 (38), 613 (34), 586 (28), 408 (45), 392 (56), 356 (51), 349 (72), 333 (77), 315 (67), 274 (100), 258 (43), 202 (46), 146 (47), 130 (33), 97 (54), 87 (36). Anal. calcd for $C_{46}H_{42}N_4O_2$ (682.87): C, 80.91; H, 6.20; N, 8.20. Found: C, 81.14; H, 6.00; N, 8.00%.

*4.1.8. 1,4-Bis(4-(1-phenyl-3-(p-tolyl)-4,5-dihydro-1H-pyrazol-5-yl)phenoxy)butane (**5bb**).* Off-white solid, 70% yield; mp 220−222 °C; IR (KBr): v 3032, 2924 (C−H), 1388, 1242, 1172, 1111 (4CH_2) cm^{-1}; ^{1}H NMR (DMSO-d_6): δ 1.79 (t, 4H, 2CH_2), 2.33 (s, 6H, 2CH_3), 3.05 (t, 2H, CH, pyrazoline-H), 3.94 (t, 4H, 2CH_2O), 5.32 (t, 2H, 2CH, pyrazoline-H), 6.65−7.63 (m, 26H, Ar−H) ppm; MS m/z (%): 714 (M^+, 39), 688 (28), 632 (35), 604 (80), 587 (100), 574 (41), 502 (65), 452 (38), 413 (71), 393 (47), 327 (24), 256 (47), 230 (79), 219 (85), 213 (64), 186 (39), 135 (27). Anal. calcd for $C_{48}H_{46}N_4O_2$ (714.87): C, 81.11; H, 6.52; N, 7.88. Found: C, 77.60; H, 5.60; N, 8.11%.

*4.1.9. 1,4-Bis(4-(3-(4-chlorophenyl)-1-phenyl-4,5-dihydro-1H-pyrazol-5-yl)phenoxy)butane (**5bd**).* Off-white solid, 83% yield; mp 200−202 °C; IR (KBr): v 3032, 2931 (C−H), 1388, 1242, 1172, 1064 (4CH_2) cm^{-1}; ^{1}H NMR (DMSO-d_6): δ 1.80 (t, 4H, 2CH_2), 3.08 (t, 2H, CH, pyrazoline-H), 3.86 (t, 4H, 2CH_2O), 5.45 (t, 2H, 2CH, pyrazoline-H), 6.68−7.76 (m, 26H, Ar−H) ppm; MS m/z (%): 755 (M^+, 7), 727 (15), 654 (12), 642 (12), 590 (12), 569 (24), 470 (22), 421 (12), 386 (24), 363 (78), 317 (100), 281 (23), 260 (23), 160 (21), 67 (33), 43 (38), 40 (50). Anal. calcd for $C_{46}H_{40}Cl_2N_4O_2$ (751.75): C, 73.50; H, 5.36; N, 7.45. Found: C, 73.75; H, 5.10; N, 7.19%.

*4.1.10. 1,4-Bis(4-(3-(4-bromophenyl)-1-phenyl-4,5-dihydro-1H-pyrazol-5-yl)phenoxy)butane (**5bf**).* Off-white solid, 80% yield; mp 179−180 °C; IR (KBr): v 3055, 2932 (C−H), 1319, 1242, 1172, 1064 (4CH_2) cm^{-1}; ^{1}H NMR (DMSO-d_6): δ 1.91 (t, 4H, 2CH_2), 3.03 (t, 2H, CH, pyrazoline-H), 3.95 (t, 4H, 2CH_2O), 5.44 (t, 2H, 2CH, pyrazoline-H), 6.68−7.86 (m, 26H, Ar−H) ppm; MS m/z (%): 840 (M^+, 28), 791 (34), 710 (44), 685 (67), 670 (35), 578 (50), 530 (27), 434 (39), 310 (36), 232 (44), 194 (38), 162 (30), 89 (100), 58 (39), 43 (44). Anal. calcd for $C_{46}H_{40}Br_2N_4O_2$ (840.66): C, 65.73; H, 4.80; N, 6.66. Found: C, 65.93; H, 4.61; N, 6.46%.

*4.1.11. 1,4-Bis(4-(3-(4-nitrophenyl)-1-phenyl-4,5-dihydro-1H-pyrazol-5-yl)phenoxy)butane (**5bh**).* Off-white solid, 72% yield; mp 240−242 °C; IR (KBr): v 3085, 2939 (C−H), 1396, 1242, 1172, 1118 (4CH_2) cm^{-1}; ^{1}H NMR (DMSO-d_6): δ 1.79 (t, 4H, 2CH_2), 3.36 (t, 4H, 2CH_2O), 5.44 (t, 2H, 2CH, pyrazoline-H), 6.69−8.18 (m, 26H, Ar−H) ppm; ^{13}C NMR (DMSO-d_6): δ 25.8, 43.2 (2CH_2), 63.2, 67.4 (2OCH_2), 113.5, 115.3, 119.2, 127.5, 127.7, 129.1, 129.3, 131.7, 133.4, 134.6, 144.4, 146.5, 158.3 (Ar−H) ppm; MS m/z (%): 772 (M^+, 24), 762 (39), 720 (18), 657 (15), 599 (18), 530 (16), 502 (12), 419 (38), 407 (32), 378 (65), 351 (100), 340 (31), 317 (32), 288 (54), 286 (77), 264 (59), 245(67), 233 (46), 220 (53), 187 (78), 93 (37), 67 (52). Anal. calcd for $C_{46}H_{40}N_6O_6$ (772.86): C, 71.49; H, 5.22; N, 10.87. Found: C, 71.73; H, 5.00; N, 10.68%.

*4.2. General Procedure for the Synthesis of Bis-chalcone Derivatives **8a−j**.* To a stirred mixture of bis-acetophenone **6** (10 mmol) and benzaldehyde derivatives **7a−j** (20 mmol) in ethanol (50 mL), NaOH (0.30 g, 60 mmol) was added slowly. The reaction mixture was stirred at 60−70 °C for 2−4 h and then left to cool to ambient temperature. The solvent was removed by filtration, washed with water (20 mL), and air-dried. The resulting solid was recrystallized from dioxane to afford the corresponding bis(chalcones) derivative **8a−j**.

*4.2.1. 1,1′-((Butane-1,4-diylbis(oxy))bis(4,1-phenylene))-bis(3-(3,5-dimethoxyphenyl)prop-2-en-1-one) (**8d**).* White solid, 60% yield; mp 169−170 °C; IR (KBr): v 3068, 2926 (C−H), 1651 (2C═O), 1256, 1214, 1167, 1134 (4CH_2) cm^{-1}; ^{1}H NMR (DMSO-d_6): δ 1.91 (t, 4H, 2CH_2), 3.81 (s, 6H, 2OCH_3), 3.85 (s, 6H, 2OCH_3), 4.16 (t, 4H, 2CH_2), 7.00 (d, J = 9, 2H, CH), 7.34−7.92 (m, 14H, Ar−H); 8.13 (d, J = 9, 2H, CH) ppm; MS m/z (%): 622 (M^+, 25), 600 (42), 556 (15), 407 (81), 378 (36), 353 (52), 351 (100), 329 (89), 317 (88), 268 (63), 159 (28), 98 (35), 71 (51). Anal. calcd for $C_{38}H_{38}O_8$ (622.71): C, 73.29; H, 6.16. Found: C, 73.55; H, 5.90%.

*4.2.2. 1,1′-((Butane-1,4-diylbis(oxy))bis(4,1-phenylene))-bis(3-(4-bromophenyl)prop-2-en-1-one) (**8g**).* White solid, 85% yield; mp 210−212 °C; IR (KBr): v 3067, 2947 (C−H), 1659 (2C═O), 1253, 1221, 1175, 1111 (4CH_2) cm^{-1}; ^{1}H NMR (DMSO-d_6): δ 1.91 (t, 4H, 2CH_2), 4.14 (t, 4H, 2CH_2), 7.06 (d, J = 9, 2H, CH), 7.03−7.98 (m, 16H, Ar−H), 8.14 (d, J = 9, 2H, CH) ppm; MS m/z (%): 660 (M^+, 8), 655 (3), 535 (21), 407 (33), 366 (17), 347 (100), 331 (31), 317 (70), 274 (24), 261 (16), 240 (13), 180 (13), 126 (35), 68 (28), 43 (31). Anal. calcd for $C_{34}H_{28}Br_2O_4$ (660.41): C, 61.83; H, 4.26. Found: C, 62.11; H, 4.00%.

*4.2.3. 1,1′-((Butane-1,4-diylbis(oxy))bis(4,1-phenylene))-bis(3-(2,4-dichlorophenyl)prop-2-en-1-one) (**8h**).* Off-white solid, 80% yield; mp 188−190 °C; IR (KBr): v 3045, 2956 (C−H), 1655 (2C═O), 1252, 1216, 1170, 1133 (4CH_2) cm^{-1}; ^{1}H NMR (DMSO-d_6): δ 1.91 (t, 4H, 2CH_2), 4.16 (t, 4H, 2CH_2), 7.08 (d, J = 9, 2H, CH), 7.52−7.98 (m, 14H, Ar−H), 8.15 (d, J = 9, 2H, CH) ppm; MS m/z (%): 640 (M^+, 20), 627 (100), 613 (35), 592 (74), 550 (52), 513 (78), 452 (48), 410 (66), 371 (59), 316 (40), 230 (46), 214 (37), 101 (41), 44 (47). Anal. calcd for $C_{34}H_{26}Cl_4O_4$(640.38): C, 63.77; H, 4.09. Found: C, 63.99; H, 3.86%

*4.2.4. 1,1′-((Butane-1,4-diylbis(oxy))bis(4,1-phenylene))-bis(3-(4-nitrophenyl)prop-2-en-1-one) (**8i**).* Yellow solid, 71% yield; mp 215−216 °C; IR (KBr): v 3043, 2920 (C−H), 1689 (2C═O), 1260, 1211, 1172, 1115 (4CH_2) cm^{-1}; ^{1}H NMR (DMSO-d_6): δ 1.91 (t, 4H, 2CH_2), 4.19 (t, 4H, 2CH_2), 7.12 (d, J = 9, 2H, CH), 7.73−8.19 (m, 14H, Ar−H), 8.25 (d, J = 9, 2H, CH) ppm; MS m/z (%): 592 (M^+, 17), 523 (48), 466 (15), 436 (76), 320 (40), 317 (35), 294 (100), 240 (25), 203 (45), 187 (74), 130 (28), 68 (47). Anal. calcd for $C_{34}H_{28}N_2O_8$ (592.61): C, 68.90; H, 4.77; N, 4.72. Found: C, 69.18; H, 4.49; N, 4.50%.

https://doi.org/10.1021/acsomega.3c06348
ACS Omega 2024, 9, 3349−3362

*4.2.5. 1,1′-((Butane-1,4-diylbis(oxy))bis(4,1-phenylene))-bis(3-(furan-2-yl)prop-2-en-1-one) (**8j**).* Off-white solid, 80% yield; mp 160−162 °C; IR (KBr): ν 3065, 2956 (C−H), 1655 (2C═O), 1252, 1218, 1179, 1135 ($4CH_2$) cm^{-1}; ^1H NMR (DMSO-d_6): δ 1.92 (t, 4H, $2CH_2$), 4.16 (t, 4H, $2CH_2$), 6.66 (d, *J* = 9, 2H, CH), 7.06−7.88 (m, 14H, Ar−H), 8.03 (d, *J* = 9, 2H, CH) ppm; MS *m*/*z* (%): 482 (M^+, 19), 468 (38), 459 (89), 452 (79), 449 (42), 411 (34), 392 (74), 382 (66), 376 (66), 333 (50), 241 (41), 193 (39), 146 (64), 133 (57), 121 (97), 115 (100), 102 (62), 91 (65), 74 (98). Anal. calcd for $C_{30}H_{26}O_6$ (482.53): C, 74.67; H, 5.43. Found: C, 74.86; H, 5.18%.

*4.3. General Procedure for the Synthesis of Bis-pyrazoline Derivatives **9a(d, g-j)** and **9b(d, g-j)**.* A solution of bis-chalcone derivatives **8a(d, g-j)** (10 mmol) and hydrazine hydrate **4a** or phenyl hydrazine **4b** (20 mmol) in ethanol (50 mL) was refluxed with stirring for 6 h. The mixture was cooled to ambient temperature, and the formed solid was filtered off. The solid was washed with ethanol (20 mL) and was allowed to dry at room temperature. The obtained solid was recrystallized from DMF to afford the corresponding bis-pyrazoline derivative **9a(d, g-j)** and **9b(d, g-j)**.

*4.3.1. 1,4-Bis(4-(3-(3,5-dimethoxyphenyl)-4,5-dihydro-1H-pyrazol-5-yl)phenoxy)butane (**9ad**).* Off-white solid, 72% yield; mp 159−160 °C; IR (KBr): ν 3340 (2NH), 3039, 2931 (C−H), 1303, 1249, 1172, 1026 ($4CH_2$) cm^{-1}; ^1H NMR (DMSO-d_6): δ 1.91 (t, 4H, $2CH_2$), 3.84 (t, 2H, CH, pyrazoline-H), 4.15 (t, 4H, $2CH_2$), 4.81−4.78 (t, 4H, $2CH_2$, pyrazoline), 6.93−8.14 (m, 14H, Ar−H), 7.16 (s, 2H, 2NH) ppm; ^{13}C NMR (DMSO-d_6): δ 25.8 ($2CH_2$), 63.8, 67.5 ($2OCH_2$), 70.3, 75.7 ($2OCH_3$), 126.2, 128.5, 129.0, 130.3, 131.1, 132.2, 135.8, 148.5, 156.6 (Ar−H) ppm; MS *m*/*z* (%): 650 (M^+, 35), 608 (20), 589 (60), 577 (48), 531 (64), 514 (41), 433 (51), 400 (76), 350 (34), 283 (40), 251 (39), 220 (73), 185 (50), 148 (41), 80 (51), 60 (100), 57 (99). Anal. calcd for $C_{38}H_{42}N_4O_6$ (650.78): C, 70.13; H, 6.51; N, 8.61. Found: C, 70.40; H, 6.29; N, 8.38%.

*4.3.2. 1,4-Bis(4-(3-(4-bromophenyl)-4,5-dihydro-1H-pyrazol-5-yl)phenoxy)butane (**9ag**).* Light green solid, 71% yield; mp 258−260 °C; IR (KBr): ν 3340 (2NH), 3062, 2947 (C−H), 1396, 1249, 1172, 1111 ($4CH_2$) cm^{-1}; ^1H NMR (DMSO-d_6): δ 1.92 (t, 4H, $2CH_2$), 3.16 (t, 2H, CH, pyrazoline-H), 4.08 (t, 4H, $2CH_2$), 4.75 (t, 4H, $2CH_2$, pyrazoline), 7.01−8.16 (m, 16H, Ar−H), 7.97 (s, 2H, 2NH) ppm; ^{13}C NMR (DMSO-d_6): δ 23.6 ($2CH_2$), 64.8, 68.5 ($2OCH_2$), 115.1, 127.5, 128.2, 128.9, 129.1, 130.0, 132.7, 133.7, 134.2, 148.5, 158.0 (Ar−H) ppm; MS *m*/*z* (%): 688 (M^+, 59), 667 (25), 549 (20), 518 (20), 485 (69), 444 (20), 403 (20), 364 (60), 340 (40), 329 (36), 281 (47), 257 (60), 225 (37), 202 (66), 171 (100), 147 (39), 114 (43), 98 (35), 77 (61). Anal. calcd for $C_{34}H_{32}Br_2N_4O_2$ (688.46): C, 59.32; H, 4.69; N, 8.14. Found: C, 59.51; H, 4.44; N, 8.00%.

*4.3.3. 1,4-Bis(4-(3-(2,4-dichlorophenyl)-4,5-dihydro-1H-pyrazol-5-yl)phenoxy)butane (**9ah**).* Light green solid, 75% yield; mp 220−222 °C; IR (KBr): ν 3332 (2NH), 3062, 2947 (C−H), 1303, 1249, 1172, 1095 ($4CH_2$) $cm^{-1}$$^1H$ NMR (DMSO-d_6): δ 1.90 (t, 4H, $2CH_2$), 3.39 (t, 2H, CH, pyrazoline-H), 4.12 (t, 4H, $2CH_2$), 4.80 (t, 4H, $2CH_2$, pyrazoline), 7.01−8.16 (m, 14H, Ar−H), 7.26 (s, 2H, 2NH) ppm; MS *m*/*z* (%): 670 (M+2, 25), 668 (M^+, 24), 608 (27), 539 (15), 519 (39), 517 (49), 457 (25), 442 (31), 421 (29), 383 (20), 339 (100), 307 (23), 174 (42), 137 (32), 86 (25), 66 (32). Anal. calcd for $C_{34}H_{30}Cl_4N_4O_2$ (668.44): C, 61.09; H, 4.52; N, 8.38. Found: C, 61.35; H, 4.30; N, 8.15%.

*4.3.4. 1,4-Bis(4-(3-(4-nitrophenyl)-4,5-dihydro-1H-pyrazol-5-yl)phenoxy)butane (**9ai**).* Off-white solid, 65% yield; mp 250−251 °C; IR (KBr): ν 3340 (NH), 3101, 2939 (C−H), 1303, 1294, 1172, 1111 ($4CH_2$) cm^{-1}; ^1H NMR (DMSO-d_6): δ 1.87 (t, 4H, $2CH_2$), 2.83 (t, 2H, CH, pyrazoline-H), 4.01 (t, 4H, $2CH_2$), 4.77−4.82 (t, 4H, $2CH_2$, pyrazoline), 6.89−8.18 (m, 16H, Ar−H), 10.21 (s, 2H, 2NH) ppm; ^{13}C NMR (DMSO-d_6): δ 25.8 ($2CH_2$), 63.8, 67.5 ($2OCH_2$), 114.8, 127.4, 128.2, 128.7, 128.9, 130.3, 132.7, 132.9, 135.1, 147.8, 158.3 (Ar−H) ppm; MS *m*/*z* (%): 620 (M^+, 23), 554 (46), 503 (17), 493 (22), 440 (72), 362 (65), 349 (86), 347 (67), 317 (100), 278 (76), 236 (50), 210 (54), 185 (40), 135 (29), 75 (67), 44 (52). Anal. calcd for $C_{34}H_{32}N_6O_6$ (620.67): C, 65.80; H, 5.21; N, 13.53. Found: C, 66.00; H, 5.00; N, 13.35%.

*4.3.5. 1,4-Bis(4-(3-(furan-2-yl)-4,5-dihydro-1H-pyrazol-5-yl)phenoxy)butane (**9aj**).* Pel green, solid, 68% yield; mp 270−271 °C;IR (KBr): ν 3325 (2NH), 3070, 2954 (C−H), 1350, 1249, 1172, 1049 ($4CH_2$) cm^{-1}; ^1H NMR (DMSO-d_6): δ 1.91 (t, 4H, $2CH_2$), 3.15 (t, 2H, CH, pyrazoline-H), 4.14 (t, 4H, $2CH_2$), 4.57 (t, 4H, $2CH_2$, pyrazoline), 6.74−8.03 (m, 14H, Ar−H), 6.84 (s, 2H, 2NH) ppm; MS *m*/*z* (%): 510 (M^+, 54), 502 (26), 488 (28), 426 (43), 406 (48), 392 (42), 350 (70), 335 (52), 328 (58), 304 (37), 288 (78), 265 (66), 231 (40), 202 (31), 192 (37), 176 (43), 152 (57), 130 (37), 98 (39), 43 (100). Anal. calcd for $C_{30}H_{30}N_4O_4$ (510.60): C, 70.57; H, 5.92; N, 10.97. Found: C, 70.86; H, 5.68; N, 10.70%.

*4.3.6. 1,4-Bis(4-(3-(3,5-dimethoxyphenyl)-1-phenyl-4,5-dihydro-1H-pyrazol-5-yl)phenoxy)butane (**9bd**).* Off-white solid, 72% yield; mp 226−228 °C; IR (KBr): ν 3047, 2924 (C−H), 1381, 1319, 1249, 1172 ($4CH_2$) cm^{-1}; MS *m*/*z* (%): 803 (M^+, 18), 772 (19), 656 (18), 585 (20), 550 (29), 505 (15), 380 (50), 363 (100), 337 (40), 330 (35), 310 (30), 282 (31), 233 (82), 178 (47), 68 (34), 62 (83). Anal. calcd for $C_{50}H_{50}N_4O_6$ (802.97): C, 74.79; H, 6.29; N, 6.98. Found: C, 74.99; H, 6.10; N, 6.81%.

*4.3.7. 1,4-Bis(4-(3-(4-bromophenyl)-1-phenyl-4,5-dihydro-1H-pyrazol-5-yl)phenoxy)butane (**9bg**).* Off-white solid, 70% yield; mp 170−172 °C; IR (KBr): ν 3062, 2954 (C−H), 1388, 1319, 1249, 1172 ($4CH_2$) cm^{-1}; ^1H NMR (DMSO-d_6): δ 1.92 (t, 4H, $2CH_2$), 4.08 (t, 4H, $2CH_2O$), 4.90 (t, 2H, 2CH, pyrazoline-H), 7.00−8.16 (m, 26H, Ar−H) ppm; MS *m*/*z* (%): 841 (M^+, 13), 814 (27), 781 (25), 762 (35), 659 (31), 638 (22), 573 (14), 522 (22), 495 (29), 409 (46), 395 (59), 377 (94), 370 (45), 363 (84), 347 (57), 327 (52), 316 (100), 271 (78), 239 (91). Anal. calcd for $C_{46}H_{40}Br_2N_4O_2$ (840.66): C, 65.72; H, 4.80; N, 6.66. Found: C, 65.95; H, 4.64; N, 6.49%.

*4.3.8. 1,4-Bis(4-(3-(2,4-dichlorophenyl)-1-phenyl-4,5-dihydro-1H-pyrazol-5-yl)phenoxy)butane (**9bh**).* Pale yellow solid, 65% yield; mp 165−166 °C; IR (KBr): ν 3047, 2954 (C−H), 1388, 1319, 1249, 1172 ($4CH_2$) cm^{-1}; ^1H NMR (DMSO-d_6): δ 1.93 (t, 4H, $2CH_2$), 4.08 (t, 4H, $2CH_2O$), 5.55 (t, 2H, 2CH, pyrazoline-H), 6.85−8.24 (m, 24H, Ar−H) ppm; MS *m*/*z* (%): 822 (M^+, 30), 804 (42), 790 (52), 769 (58), 759 (56), 735 (100), 715 (35), 701 (37), 678 (33), 670 (34), 634 (75), 564 (34), 542 (44), 514 (34), 489 (35), 458 (59). Anal. calcd for $C_{46}H_{38}Cl_4N_4O_2$ (820.65): C, 67.33; H, 4.67; N, 6.83. Found: C, 67.55; H, 4.50; N, 6.55%.

*4.3.9. 1,4-Bis(4-(3-(4-nitrophenyl)-1-phenyl-4,5-dihydro-1H-pyrazol-5-yl)phenoxy)butane (**9bi**).* Pale yellow solid, 60% yield; mp 235−236 °C; IR (KBr): ν 3076, 2939 (C−H), 1396, 1242, 1172, 1111 ($4CH_2$) cm^{-1}; ^1H NMR (DMSO-d_6): δ 1.90 (t, 4H, $2CH_2$), 4.12 (t, 4H, $2CH_2O$), 4.60 (t, 2H, 2CH, pyrazoline-H), 7.00−8.18 (m, 26H, Ar−H) ppm; MS *m*/*z* (%): 773 (M^+, 9), 764 (63), 702 (32), 667 (81), 603 (20), 556 (42), 521 (37), 436 (26), 412 (81), 388 (24), 343 (69), 323 (47), 304

https://doi.org/10.1021/acsomega.3c06348
ACS Omega 2024, 9, 3349−3362

(56), 274 (74), 243 (64), 217 (100), 166 (35), 150 (42), 82 (25). Anal. calcd for $C_{46}H_{40}N_6O_6$ (772.86): C, 71.49; H, 5.22; N, 10.87. Found: C, 71.70; H, 5.00; N, 10.65%.

*4.3.10. 1,4-Bis(4-(3-(furan-2-yl)-1-phenyl-4,5-dihydro-1H-pyrazol-5-yl)phenoxy)butane (**9bj**).* Off-white solid, 66% yield; mp 204−205 °C; IR (KBr): ν 3047, 2924 (C−H), 1388, 1219, 1172, 1011 ($4CH_2$) cm^{-1}; ^1H NMR (DMSO-d_6): δ 1.90 (t, 4H, $2CH_2$), 3.63 (t, 4H, $2CH_2O$), 5.49 (t, 2H, 2CH, pyrazoline-H), 6.36−7.71 (m, 26H, Ar−H) ppm; MS *m*/*z* (%): 663 (M^+, 26), 626 (100), 556 (14), 527 (17), 489 (17), 472 (46), 420 (42), 371 (14), 340 (16), 364 (16), 240 (10), 206 (10), 177 (17). Anal. Calcd for $C_{42}H_{38}N_4O_4$ (662.79): C, 76.11; H, 5.78; N, 8.45. Found: C, 76.30; H, 5.68; N, 8.31%.

4.4. Biological Activities. *4.4.1. Cytotoxicity Evaluation.* Th cytotoxicity screening was accomplished using normal human lung fibroblast cells (WI-38 cell line, American Type Culture Collection, ATCC, Rockville, MD).

Crystal violet stain solution (1%) was made using 0.5% (w/v) crystal violet (Sigma, St. Louis, MO) and 50% methanol, and then the mixture was made up to volume with double distilled water and filtered through a Whatman No.1 filter paper. The cells were reproduced in Dulbecco's modified Eagle's medium (DMEM, Lonza) accompanied by 10% heat-inactivated fetal bovine serum (Lonza), 1% L-glutamine (Lonza), HEPES buffer (Lonza), and 50 μg/mL gentamycin (Lonza). All cells were preserved at 37 °C in a humidified atmosphere with 5% CO_2 and were subcultured twice a week. For the cytotoxicity assay, the cells were seeded in a 96-well plate at a cell concentration of 1×10^4 cells per well in 100 μL of growth medium. A fresh medium including different concentrations of the test sample was added after 24 h of seeding. Serial twofold dilutions of the test compounds were added to confluent cell monolayers dispensed into 96-well, flat-bottomed microtiter plates (Falcon, NJ) using a multichannel pipet. The microtiter plates were kept at 37 °C in a humidified incubator with 5% CO_2 for a period of 24 h. Three wells were used for each concentration of the test sample. Control cells were incubated without a test sample and with or without DMSO (Sigma, St. Louis, Mo). The small percentage of DMSO present in the wells (maximal 0.1%) did not have any significant effect on the experiment. Following cells' incubation, viable cells' yield was determined by colorimetric techniques.[37,38]

The media were collected after the period, and the 1% crystal violet solution was added to the wells for ≥30 min. The excess crystal violet stain was totally removed *via* rinsing the plates with tap water. Thereafter, a solution of 30% acetic acid was added, and the wells were gently shaken prior to absorbance measurement at 490 nm (Microplate reader, TECAN, Inc.) against a blank solution prepared simultaneously without the addition of the stain. Control samples were made, where the test compounds were absent, for comparison with the treated samples. The experiments were repeated three times to allow for statistical evaluation of the obtained data. Additionally, the microplate reader was used to determine the optical density of the samples so as to measure the percent cell viability from eq 1:[37] %viability = $[OD_t/OD_c] \times 100$, where OD_t is the mean optical density of wells treated with the test sample and OD_c is the mean optical density of the untreated cells. The number of surviving cells was plotted against the drug concentration in order to acquire the survival correlation of each tumor cell line after treatment with the test compounds. The concentration required to cause a toxic effect on 50% of the intact cells (cytotoxic concentration, CC_{50}) was calculated from the dose−response curve for each measurement.

4.5. *In Silico* Study. The 2D structures of the prepared molecules were generated in cdx format. The produced SMILES were applied as input to obtain the 3D structures of the synthesized compounds by utilizing Open Babel GUI 2.4.1 tool.[39] The 3D conformation of the target enzyme was obtained from Protein data bank (PDB ID: 2x3f).[40] The target file was optimized by removing the cocrystallized ligands and water molecules. Their energies were minimized using UFF force field[41] in PyRx tool and CHARMm Force Field[42] in Discovery Studio 3.5 Visualizer, respectively. All of the synthesized analogues were docked into the active sites of the targets. The docking simulations were performed using the Lamarckian genetic algorithm (LGA).[43] The best enzyme−ligand complexes were ranked based on the binding energy of the docked complex. Additionally, electrostatic potential (ESP) map was obtained using Gaussian 03 program.[44] Moreover, the ADMET analysis of the compounds was achieved to check whether they have drug-like properties or not using SwissADME and Mol inspiration web servers.

■ ASSOCIATED CONTENT

Supporting Information

The Supporting Information is available free of charge at https://pubs.acs.org/doi/10.1021/acsomega.3c06348.

Spectral data of compounds **5aa-5bh**; spectral data of compounds **8a−8j**, and spectral data of compounds **9ad-9bj** (PDF)

■ AUTHOR INFORMATION

Corresponding Authors

Refaie M. Kassab − *Department of Chemistry, Faculty of Science, Cairo University, Giza 12613, Egypt*; orcid.org/0000-0002-8304-736X; Email: rkassab@sci.cu.edu.eg

Sami A. Al-Hussain − *Department of Chemistry, Faculty of Science, Imam Mohammad Ibn Saud Islamic University (IMSIU), Riyadh 11623, Saudi Arabia*; Phone: +20-01013362594; Email: sahussain@imamu.edu.sa; Fax: +2-025-685-799

Zeinab A. Muhammad − *Pharmaceutical Chemistry Department, National Organization for Drug Control and Research (NODCAR), Giza 12311, Egypt*; orcid.org/0000-0003-1711-8497; Email: zeinab.a.muhammad@gmail.com

Authors

Magdi E. A. Zaki − *Department of Chemistry, Faculty of Science, Imam Mohammad Ibn Saud Islamic University (IMSIU), Riyadh 11623, Saudi Arabia*

Aboubakr H. Abdelmonsef − *Chemistry Department, Faculty of Science, South Valley University, Qena 83523, Egypt*; orcid.org/0000-0002-4616-0224

Complete contact information is available at: https://pubs.acs.org/10.1021/acsomega.3c06348

Notes

The authors declare no competing financial interest.

https://doi.org/10.1021/acsomega.3c06348
ACS Omega 2024, 9, 3349−3362

■ ACKNOWLEDGMENTS

The authors are indebted to the generous support of the Deanship of Scientific Research, Imam Mohammad Ibn Saud Islamic University, Saudi Arabia.

■ REFERENCES

(1) Nehra, B.; Rulhania, S.; Jaswal, S.; Kumar, B.; Singh, G.; Monga, V. Recent advancements in the development of bioactive pyrazoline derivatives. *Eur. J. Med. Chem.* **2020**, *205*, No. 112666.
(2) Manna, K.; Banik, U.; Ghosh, P. S.; Das, M. A Review on Synthesis and Pharmacological Diversity of Isoxazoles & Pyrazolines. *Nirma Univ. J. Pharm. Sci.* **2014**, *1*, 37−49.
(3) Monga, V.; Goyal, K.; Steindel, M.; Malhotra, M.; Rajani, D. P.; Rajani, S. D. Synthesis and evaluation of new chalcones, derived pyrazoline and cyclohexenone derivatives as potent antimicrobial, antitubercular and antileishmanial agents. *Med. Chem. Res.* **2014**, *23* (4), 2019−2032.
(4) Hassan, S. Y. Synthesis, antibacterial and antifungal activity of some new pyrazoline and pyrazole derivatives. *Molecules* **2013**, *18* (3), 2683−2711.
(5) Wanare, G.; Aher, R.; Kawathekar, N.; Ranjan, R.; Kaushik, N. K.; Sahal, D. Synthesis of novel α-pyranochalcones and pyrazoline derivatives as Plasmodium falciparum growth inhibitors. *Bioorg. Med. Chem. Lett.* **2010**, *20* (15), 4675−4678.
(6) Bhat, A. R.; Athar, F.; Azam, A. Bis-pyrazolines: Synthesis, characterization and antiamoebic activity as inhibitors of growth of Entamoeba histolytica. *Eur. J. Med. Chem.* **2009**, *44* (1), 426−431.
(7) Kharbanda, C.; Alam, M. S.; Hamid, H.; et al. Synthesis and evaluation of pyrazolines bearing benzothiazole as anti-inflammatory agents. *Bioorg. Med. Chem.* **2014**, *22* (21), 5804−5812.
(8) Yang, W.; Hu, Y.; Yang, Y. S.; et al. Design, modification and 3D QSAR studies of novel naphthalin-containing pyrazoline derivatives with/without thiourea skeleton as anticancer agents. *Bioorg. Med. Chem.* **2013**, *21* (5), 1050−1063.
(9) Prasad, Y. R.; Rao, A. L.; Prasoona, L.; Murali, K.; Kumar, P. R. Synthesis and antidepressant activity of some 1,3,5-triphenyl-2-pyrazolines and 3-(2″-hydroxy naphthalen-1″-yl)-1,5-diphenyl-2-pyrazolines. *Bioorg. Med. Chem. Lett.* **2005**, *15* (22), 5030−5034.
(10) Bhandari, S.; Tripathi, A. C.; Saraf, S. K. Novel 2-pyrazoline derivatives as potential anticonvulsant agents. *Med. Chem. Res.* **2013**, *22* (11), 5290−5296.
(11) Ali, M. A.; Shaharyar, M.; Siddiqui, A. A. Synthesis, structural activity relationship and anti-tubercular activity of novel pyrazoline derivatives. *Eur. J. Med. Chem.* **2007**, *42* (2), 268−275.
(12) Lv, P. C.; Li, D. D.; Li, Q. S.; Lu, X.; Xiao, Z. P.; Zhu, H. L. Synthesis, molecular docking and evaluation of thiazolyl-pyrazoline derivatives as EGFR TK inhibitors and potential anticancer agents. *Bioorg. Med. Chem. Lett.* **2011**, *21* (18), 5374−5377.
(13) Lange, J. H. M.; Attali, A.; van der Neut, M. A. W.; et al. Two distinct classes of novel pyrazolinecarboxamides as potent cannabinoid CB1 receptor agonists. *Bioorg. Med. Chem. Lett.* **2010**, *20* (17), 4992−4998.
(14) Yang, G. Y.; Oh, K.-A.; Park, N.-J.; Jung, Y.-S. New oxime reactivators connected with CH2O(CH2)nOCH2 linker and their reactivation potency for organophosphorus agents-inhibited acetylcholinesterase. *Bioorg. Med. Chem.* **2007**, *15* (24), 7704−7710.
(15) Holla, B. S.; Gonsalves, R.; Shenoy, S. Synthesis and antibacterial studies of a new series of 1,2-bis(1,3,4- oxadiazol-2-yl)ethanes and 1,2-bis(4-amino-1,2,4-triazol-3-yl)ethanes. *Eur. J. Med. Chem.* **2000**, *35* (2), 267−271.
(16) Kassab, R. M.; Gomha, S. M.; Muhammad, Z. A.; El-khouly, A. S. Synthesis, Biological Profile, and Molecular Docking of Some New Bis-Imidazole Fused Templates and Investigation of their Cytotoxic Potential as Anti-tubercular and/or Anticancer Prototypes. *Med. Chem.* **2021**, *17* (8), 875−886.
(17) Kassab, R. M.; Khalil, F. S. A. M.; Abbas, A. A. Synthesis and Antimicrobial Activities of Some New Bis(Schiff Bases) and Their Triazole-Based Lariat Macrocycles. *Polycyclic Aromat. Compd.* **2022**, *42* (5), 2751−2766.
(18) Kassab, R. M.; Gomha, S. M.; Al-Hussain, S. A.; et al. Synthesis and in-silico studies of new bis-thiazole derivatives and their preliminary antimicrobial activity. *Arab. J. Chem.* **2021**, *14*, No. 103396.
(19) Mahmoud, H. K.; Kassab, R. M.; Gomha, S. M. Synthesis and characterization of some novel bis-thiazoles. *J. Heterocycl. Chem.* **2019**, *56* (11), 3157−3163.
(20) Barsoum, F. F.; Hosni, H. M.; Girgis, A. S. Novel bis(1-acyl-2-pyrazolines) of potential anti-inflammatory and molluscicidal properties. *Bioorg. Med. Chem.* **2006**, *14* (11), 3929−3937.
(21) Srivastava, S.; Joshi, S.; Singh, A. R.et al. Oxygenated Chalcones and Bischalcones as a New Class of Inhibitors of DNA Topoisomerase II of Malarial Parasites. In *Medicinal Chemistry Research*; Springer, 2008; pp 234−244.
(22) Yusuf, M.; Jain, P. New bispyrazoline derivatives built around aliphatic chains: Synthesis, characterization and antimicrobial studies. *J. Chem. Sci.* **2013**, *125* (1), 117−127.
(23) Yusuf, M.; Kaur, A.; Abid, M. Synthesis, Antimicrobial Studies, and Docking Simulations of New Bis(4,5-dihydropyrazole) Derivatives. *J. Heterocycl. Chem.* **2017**, *54* (4), 2536−2547.
(24) Barsoum, F. F.; Girgis, A. S. Facile synthesis of bis(4,5-dihydro-1H-pyrazole-1-carboxamides) and their thio-analogues of potential PGE2 inhibitory properties. *Eur. J. Med. Chem.* **2009**, *44* (5), 2172−2177.
(25) Liargkova, T.; Hadjipavlou-Litina, D. J.; Koukoulitsa, C.; Voulgari, E.; Avgoustakis, C. Simple chalcones and bis -chalcones ethers as possible pleiotropic agents. *J. Enzyme Inhib. Med. Chem.* **2016**, *31* (2), 302−313.
(26) Dhar, D. N. *The Chemistry of Chalcones and Related Compounds*; John Wiley & Sons, Ltd, 1981.
(27) Harborne, J. B. *Methods in Plant Biochemistry*; Academic Press Ltd., 1989.
(28) Jovanovic, S. V.; Steenken, S.; Tosic, M.; Marjanovic, B.; Simic, M. G. Flavonoids as antioxidants. *J. Am. Chem. Soc.* **1994**, *116* (11), 4846−4851.
(29) Wu, J.; Wang, C.; Cai, Y.; et al. Synthesis and crystal structure of chalcones as well as on cytotoxicity and antibacterial properties. *Med. Chem. Res.* **2012**, *21* (4), 444−452.
(30) Díaz-Tielas, C.; Graña, E.; Reigosa, M. J.; Sánchez-Moreiras, A. M. Atividades Biológicas e Novas Aplicações das Chalconas. *Planta Daninha* **2016**, *34* (3), 607−616.
(31) Narender, T.; Tanvir, K.; Rao, M.; Srivastava, K.; Puri, S. K. Prenylated chalcones isolated from Crotalaria genus inhibits in vitro growth of the human malaria parasite Plasmodium falciparum. *Bioorg. Med. Chem. Lett.* **2005**, *15* (10), 2453−2455.
(32) Kassab, R. M.; Zaki, M. E. A.; Dena, A. S. A.; Al-Hussain, S. A.; Abdel-Aziz, M. M.; Muhammad, Z. A. Novel Set of Highly Substituted Bis-pyridines: Synthesis, Molecular Docking and Drug-Resistant Antibacterial Profile. *Future Med. Chem.* **2022**, *14* (24), 1881−1897.
(33) Kostakioti, M.; Hadjifrangiskou, M.; Hultgren, S. J. Bacterial biofilms: Development, dispersal, and therapeutic strategies in the dawn of the postantibiotic era. *Cold Spring Harbor Perspect. Med.* **2013**, *3* (4), No. a010306.
(34) Abdelmonsef, A. H.; Mohamed, M. E.; El-Naggar, M.; Temairk, H.; Mosallam, A. M. Novel Quinazolin-2,4-Dione Hybrid Molecules as Possible Inhibitors Against Malaria: Synthesis and in silico Molecular Docking Studies. *Front. Mol. Biosci.* **2020**, *7*, No. 105.
(35) Hassan, A.; Mubarak, F. A. F.; Shehadi, I. A.; et al. Design and biological evaluation of 3-substituted quinazoline-2,4(1H,3H)-dione derivatives as dual c-Met/VEGFR-2-TK inhibitors. *J. Enzyme Inhib. Med. Chem.* **2023**, *38* (1), No. 2189578.
(36) Abdelmonsef, A. H.; Omar, M.; Rashdan, H. R. M.; Taha, M. M.; Abobakr, A. M. Design, synthetic approach, in silico molecular docking and antibacterial activity of quinazolin-2,4-dione hybrids bearing bioactive scaffolds. *RSC Adv.* **2022**, *13* (1), 292−308.
(37) Mosmann, T. Rapid colorimetric assay for cellular growth and survival: Application to proliferation and cytotoxicity assays. *J. Immunol. Methods* **1983**, *65* (1−2), 55−63.

https://doi.org/10.1021/acsomega.3c06348
ACS Omega 2024, 9, 3349−3362

(38) Riyadh, S. M.; Gomha, S. M.; Mahmmoud, E. A.; Elaasser, M. M. Synthesis and anticancer activities of thiazoles, 1,3-thiazines, and thiazolidine using chitosan-grafted-poly(vinylpyridine) as basic catalyst. *Heterocycles* **2015**, *91* (6), 1227−1243.
(39) O'Boyle, N. M.; Banck, M.; James, C. A.; Morley, C.; Vandermeersch, T.; Hutchison, G. R. Open Babel: An Open chemical toolbox. *J. Cheminf.* **2011**, 3 (10), No. 33.
(40) Berman, H. M.; Westbrook, J.; Feng, Z.; et al. The Protein Data Bank. *Nucleic Acids Res.* **2000**, *28* (1), 235−242.
(41) Rappé, A. K.; Casewit, C. J.; Colwell, K. S.; Goddard, W. A.; Skiff, W. M. UFF, a Full Periodic Table Force Field for Molecular Mechanics and Molecular Dynamics Simulations. *J. Am. Chem. Soc.* **1992**, *114* (25), 10024−10035.
(42) Brooks, B. R.; Brooks, C. L.; Mackerell, A. D.; et al. CHARMM: The biomolecular simulation program. *J. Comput. Chem.* **2009**, *30* (10), 1545−1614.
(43) Morris, G. M.; Goodsell, D. S.; Halliday, R. S.; et al. Automated docking using a Lamarckian genetic algorithm and an empirical binding free energy function. *J. Comput. Chem.* **1998**, *19* (14), 1639−1662.
(44) Drissi, M.; Benhalima, N.; Megrouss, Y.; Rachida, R.; Chouaih, A.; Hamzaoui, F. Theoretical and experimental electrostatic potential around the m-nitrophenol molecule. *Molecules* **2015**, *20* (3), 4042−4054.

https://doi.org/10.1021/acsomega.3c06348
ACS Omega 2024, 9, 3349−3362